Hydrology and Earth System Sciences

Open Access

Discussions

HESSD

Interactive
comment

Interactive comment on "Geostatistical assessment of summertime rainfall observations in Korea based on composite precipitation and satellite water vapor data" *by* Sojung Park et al.

Sojung Park et al.

spark@ewha.ac.kr

Received and published: 7 May 2018

Reply to the Comments by Referee #2 for Manuscript hess-2018-83

Reviewer (Comments to Author):
This manuscript investigates the spatio-temporal characteristics of summer precipitation systems over the Korean peninsula through the geostatistical analysis using the combined datasets of ground observation and radar data. For the detailed analysis, they categorized the precipitation systems into four types based on the precipitation intensity (3mm/h) and ratio (20%) of precipitated stations. They found that the e-folding

distance and time of precipitation systems are clearly dependent on the precipitation area, and directional pattern of precipitation systems. Also they found that the spatial distribution of water vapor has similar characteristics with precipitation but with strong spatial correlation over much longer distance ($\sim$100 km), through the analysis of water vapor channel data of Himawari/Advanced Himawari Imager data. The results obtained in this study can be used for the detailed understanding of precipitation over South Korea. However, the manuscript should be improved in terms of additional analyses and scientific interpretation of results. Therefore, the manuscript needs to undergo a minor revision before being ready for publication in Hydrology and Earth System Sciences. Below I give some comments and suggestions that would help improving the manuscript.

$\Longrightarrow$ We appreciate the positive and valuable comments by the referee. We have substantially improved the manuscript by making some unclear statements clearer and by adding more discussions on detailed analyses and scientific interpretation, following the referee's comments. An item-by-item response to the referee's general and minor comments is provided below.

General comments:

1) *As we know that thresholds values are very important for the categorization (or clustering) precipitation systems. Please presents the background or ground of threshold values (3mm/h, 20%) used in this study.*

   $\Longrightarrow$ We agree with the referee that the threshold values are important for categorizing the precipitation systems. In order to determine the threshold values (i.e., 20% and 3 mm/h), we have performed a preliminary statistical analysis of precipitation events (see Table R1 below). In classifying the precipitation types, we used two criteria — the portion of weather stations with precipita-

tion (C1) and the station average precipitation rate (C2). We determined the threshold values when the cumulative percentage of each criterion reaches 80% (see the red lines in Table R1). For example, in terms of C1, the cumulative percentage reaches 77.1% with the portion of 10–20% and 85.0% with the portion of 20–30%; thus selecting 20% as the threshold value. In terms of C2, the cumulative percentage becomes 80.0% with 2.0–2.9 mm/h and 93.3% with 3.0–4.9 mm/h; thus choosing 3 mm/h as the threshold value. We have added the following statement at the early part of Sec. 2 in the revised manuscript.

> In order to determine the threshold values for classifying the precipitation types, we have conducted a preliminary statistical analysis on precipitation events in the period of 2011–2015 (not shown). As the precipitation events occur in a given time period and/or space interval, our precipitation data are assumed to follow the Poisson distribution, which represents a probability situation of a large number of observation with a small probability of occurrence. Many studies developed the Poisson distribution models to estimate rainfall and cluster the rainfall systems (e.g., Rodriguez-Iturbe et al., 1987; Lee et al., 2014; Barton et al., 2016; Ritschel et al., 2017). We have chosen the threshold values when the cumulative percentage of precipitation events for each criterion (i.e., C1 and C2) reached approximately 80%; thus obtaining the threshold values of 20% for C1 and 3 mm h^{-1} for C2, respectively.

2) *The domain of data mentioned in the 2 Data description is not well matched with the analysis results (e.g., Figure 1)*

$\implies$ We appreciate the referee for pointing this out, and we admit that our data description and Fig. 1 might have caused confusion. We have used the station data, as shown in Fig. 1, to classify the precipitation types (see Table

C3

R1 below); we have utilized the 1 km composite precipitation data for the precipitation analyses, including spatial correlations. We actually noticed that Fig. 1 should be updated because the station precipitation data were obtained from three observation networks with a total of 688 stations — the Automated Synoptic Observing Systems (ASOS), the Automatic Weather Stations (AWS), and Automated Agriculture Observing System (AAOS). We also noticed that the information on the radar locations and coverages would be essential because both the station and radar data were used to produce the 1 km composite precipitation data. In the revised manuscript, we modified Fig. 1 by updating the weather station locations and by including the radar locations and coverages (see Fig. R1 below). We have rewritten the text by clearly describing the data used in this study. We first modified the beginning sentences in the second paragraph of Sec. 1, with new statements in bold, as:

> "The ground-based rainfall observation data, in Korea, are collected from the Automated Synoptic Observing Systems (ASOS), the Automatic Weather Stations (AWS), **and the Automated Agriculture Observing System (AAOS)**. The observation density is about 67 km for ASOS and approximately 13 km by including AWS. **In addition, the agrometeorological observation network consists of 11 AAOS stations (Choi et al., 2015).** · · ·"

$\Longrightarrow$ We have also modified and reorganized the early part of Sec. 2, by including the step-by-step description of the method to produce the composite precipitation data, as (new sentences in bold):

> **We used the precipitation data from weather stations, shown in Fig. 1, to categorize the precipitation systems.** We classify four different precipitation types statistically based on two criteria: the portion of weather stations with precipitation (C1), and the station average precipitation rate (C2). Based on these criteria,

C4

we define four different precipitation types, as shown in Table 1: 1) Low Precipitation at a Few Points (LPFP) for C1 < 20 % and C2 < 3 mm h^{-1}; 2) Low Precipitation at Many Points (LPMP) for C1 ≥ 20 % and C2 < 3 mm h^{-1}; 3) High Precipitation at a Few Points (HPFP) for C1 < 20 % and C2 ≥ 3 mm h^{-1}; and 4) High Precipitation at Many Points (HPMP) for C1 ≥ 20 % and C2 ≥ 3 mm h^{-1}. We practically exclude the LPFP type in our analyses, i.e., the case with C1 < 20 % and C2 < 3 mm h^{-1}, because it may be less effective.

The Korea Meteorological Administration (KMA) has produced a composite precipitation data over Korea **using the data from radars, weather stations and satellites, through the following steps as described in Hwang et al. (2015): 1) remove non-precipitation echoes from the radar data using the satellite cloud type data; 2) calculate the difference between the station precipitation and the radar estimated precipitation; 3) perform the objective analysis on the precipitation difference field and on the station precipitation data; 4) correct the bias using the objectively-analyzed difference field; and 5) combine the corrected radar-estimated precipitation data and the objectively-analyzed station precipitation data to produce the composite precipitation data (in mm h^{-1}). In order to analyze the precipitation systems with high resolution and evenly distributed data, we used this composite precipitation data.** This data covers 1153 km $\times$ 1441 km over the Korean Peninsula, with a grid size of 1 km and a time resolution of 1 h. Geostatistical analyses are conducted using this composite precipitation data sets from April to October in a period of 2013–2015 to investigate the spatial and temporal characteristics of summer rainfall.

3) *The author should mention about the sensitivity of analysis results to the threshold values for the categorization of precipitation systems.*

$\implies$ As shown in Table R1, heavy precipitation systems have high locality; especially, precipitation with the highest intensity (≥ 10 mm/hr) mostly occurs in a small area with the number of stations less than 10% of total weather stations. This is consistent with the findings of Nam et al. (2014), and implies that the precipitation analysis results may depend on (be sensitive to) the threshold values. We have added the following sentence to next to the newly-added paragraph in item 1) above:

> Our preliminary statistical analysis showed that, in general, most precipitation events occur over small areas and precipitation events with high intensity rarely occur over large areas. The locality of precipitation appeared higher as the precipitation intensity were higher, in accordance with Nam et al. (2014). In particular, precipitation systems with the highest intensity (≥ 10 mm/hr) were mostly confined to a small area with the number of stations less than 10% of total weather stations. This implies that the locality feature of precipitation systems may depend on the threshold value in precipitation intensity.

4) *It will be helpful for the understanding of the single cell storms marked by X in Figures 9 and 10 if the authors presents the background for the marking.*

$\implies$ We appreciate the referee for pointing this out. We think the expression "single cell storms" is not appropriate here. We originally intended to put the "X" marks on the locations of precipitation systems with maximum intensity (precipitation rate) and strong cluster characteristics. To avoid any confusion, we have modified the captions of Figs. 9 and 10 accordingly. By reflecting the referee's suggestion in Minor comments (items 3 and 4) and

other referee's comments as well, the captions are rewritten as:

> Figure 9. **An LPMP case at 05 KST 25 August 2015:** (a) Precipitation distribution (source from https://afso.kma.go.kr/), (b) local Z(G_i), (c) local Moran's I (I_i), and (d) Z-score of I_i. **The computational domain covers the area of** $34.34 - 38.97°$ **N and** $124.25 - 130.05°$ **E. Precipitation systems with maximum intensity and strong cluster characteristics** are marked by the crosses, and the cold spots with dispersion pattern are denoted by the arrow. **Non-precipitating areas have no color shading.**
>
> Figure 10. Same as in Fig. 9 but **for an HPMP case at 17 KST 27 May 2013 and the computational domain of** $33.43 - 38.05°$**N and** $124.25 - 130.04°$**E**.

$\implies$ We have also rewritten the statement in page 10, line 11 as:

> Figure 9c depicts **several precipitation systems with maximum intensity (i.e., precipitation rate; see Fig. 9a)** in the cluster area (marked by the crosses). **These systems show the highest local Moran's I with the spatial scale of less than 30 km.** The cluster patterns were statistically significant at a significance level of 0.01 (Fig. 9d). $\cdots\cdots$ The map of local Moran's I shows that **a precipitation system with a strong cluster feature has developed**, over the southwestern sea of the Korean Peninsula, along with the successive cluster patterns **in a line type** (Fig. 10c), with a significance level of 0.01 (Fig. 10d).

Minor comments:

1) *The location of AWS is not correct in Figure 1.*

C7

$\implies$ We have redrawn Fig. 1 in the revised manuscript (see Fig. R1 below).

2) *I think that the number of y axis in Figures 5 and 8 is km. So, give the unit in Figures 5 and 8.*

$\implies$ We appreciate the referee for pointing this out. We now have explicitly given the unit (km) in the captions of Figs. 5 and 8. We also changed the name of diagram to "radar chart" from "radar diagram" to avoid any confusion. The captions of Figs. 5 and 8 are rewritten, and the cation of Fig. 8 also reflects the referee's suggestion in items 3) and 4):

Figure 5. A radar **chart** representing the directional e-folding distance **(in km)** at the mode in Fig. 3.

Figure 8. A radar **chart** representing the directional e-folding distance **(in km)** of brightness temperature of **the Himawari/AHI** water vapor band **8, 9 and 10** at the mode in the histogram of case numbers for **LPMP (solid), HPMP (dashed), and HPFP (dotted). The colors indicate autocorrelation coefficients of 0.7 (blue), 0.8 (black), and 0.9 (grey), respectively**.

3) *Figure 6. The averaged spatial autocorrelation of brightness temperature of water vapor band (a) 8, (b) 9, and (c) 10 for each precipitation $\Rightarrow$ The averaged spatial autocorrelation of brightness temperature of water vapor band (a) 8, (b) 9, and (c) 10 Himawari/AHI for each precipitation*

$\implies$ The caption of Fig. 6 is now modified following the referee's suggestion as:

Figure 6. The averaged spatial autocorrelation of brightness temperature of **the Himawari/AHI** water vapor band (a) 8, (b) 9, and (c) 10 for each precipitation type.

4) *Some index of figures are not clear (e.g., Figures 7, 8, 9, 10, and 11).*

$\implies$ We have rewritten the captions, by reflecting suggestions by other referees as well. The revised captions appear as the followings:

Figure 7. The average directional spatial autocorrelation of the brightness temperature of **the Himawari/AHI** water vapor band **8, 9 and 10** by each precipitation type **(i.e., HPFP, HPMP, and LPMP) for directions of** $0°$ **(black),** $45°$ **(blue),** $90°$ **(red), and** $135°$ **(green). The direction (angle) is measured counterclockwise from the origin-east axis (i.e.,** $0°$**).**

Figure 8. A radar **chart** representing the directional e-folding distance **(in km)** of brightness temperature of **the Himawari/AHI** water vapor band **8, 9 and 10** at the mode in the histogram of case numbers for **LPMP (solid), HPMP (dashed), and HPFP (dotted). The colors indicate autocorrelation coefficients of 0.7 (blue), 0.8 (black), and 0.9 (grey), respectively**.

Figure 9. **An LPMP case at 05 KST 25 August 2015:** (a) Precipitation distribution (source from https://afso.kma.go.kr/), (b) local Z(G_i), (c) local Moran's I (I_i), and (d) Z-score of I_i. **The computational domain covers the area of** $34.34 - 38.97°$ **N and** $124.25 - 130.05°$ **E. Precipitation systems with maximum intensity and strong cluster characteristics** are marked by the crosses, and the cold spots with dispersion pattern are denoted by the arrow. **Non-precipitating areas have no color shading.**

Figure 10. Same as in Fig. 9 but **for an HPMP case at 17 KST 27 May 2013 and the computational domain of** $33.43 - 38.05°$**N and** $124.25 - 130.04°$**E.**

Figure 11. Same as in Fig. 9 but **for an HPFP case at 05 KST 24 October 2015 and the computational domain of** $37.14 - 39.06°$**N and** $123.32 - 131.21°$**E**.

Table R1. Preliminary statistical analysis of precipitation events during 2011–2015 by two criteria —-the portion of weather stations with precipitation and the station average precipitation rate. The red lines indicate the boundaries when the cumulative percentage of precipitation events is approximately 80 %.

Figure R1. The weather station locations (blue dots) and radar locations (red plus symbols) and coverages (white area) in Korea.

References

Barton, Y., Giannakaki, P., Von Waldow, H., Chevalier, C., Pfahl, S., and Martius, O.: Clustering of regional-scale extreme precipitation events in Southern Switzerland, Mon. Wea. Rev., 144, 347–369, 2016.

Choi, S.-W., Lee, S.-J., Kim, J. Lee, B.-L., Kim, K.-R., and Choi, B.-C.: Agrometeorological observation environment and periodic report of Korea Meteorological Administration: Current status and suggestions, Korean J. Agric. For. Meteorol., 17, 144–155, doi:10.5532/KJAFM.2015.17.2.144, 2015 (in Korean with English abstract).

Lee, J., Yoon, J., and Jun, H. D.: Evaluation for the correction of radar rainfall due to the spatial distribution of raingauge network, J. Korea Soc. Hazzard Mitig., 14, 337–345, http://dx.doi.org/10.9798/KOSHAM.2014.14.6.337, 2014.

Nam, J.-E., Lee, Y. H., Ha, J.-C., and Cho, C.-H.: A study on the e-folding distance of summer precipitation using precipitation reanalysis data, in: Proceedings of the Autumn Meeting of Korean Meteorological Society, 2014, Korean Meteorol. Soc., Jeju, Korea, 13–15 October 2014, 657–658, 2014.

Ritschel, C., Ulbrich, U., Névir, P., and Rust, H. W.: Precipitation extremes on multiple timescales — Bartlett-Lewis rectangular pulse model and intensity-duration-frequency curves, Hydrol. Earth Syst. Sci., 21, 6501–6517, https://doi.org/10.5194/hess-21-6501-2017, 2017.

Rodriguez-Iturbe, I., Cox, D. R., and Isham, V.: Some models for rainfall based on stochastic point processes, Proc. R. Soc. London, Ser. A, 410, 269–288, 1987.

		The portion of weather stations with precipitation (%)											
		0-10	10-20	20-30	30-40	40-50	50-60	60-70	70-80	80-90	90-	Sum	Percentage (%)	Cumulative percentage (%)
The station average precipitation rate (mm/h)	0.1-0.9	5241	399	156	60	29	5	2	1	0	0	5893	40.0	40.0
	1.0-1.9	2238	665	383	235	148	99	57	33	18	6	3882	26.3	66.3
	2.0-2.9	891	352	262	196	109	89	48	35	29	12	2023	13.7	80.0
	3.0-4.9	765	322	224	212	159	85	77	43	49	35	1971	13.4	93.3
	5.0-9.9	317	118	116	115	76	47	35	19	18	8	869	5.9	99.2
	10.0-	61	6	19	11	14	1	0	0	0	0	112	0.8	100.0
	Sum	9513	1862	1160	829	535	326	219	131	114	61	14750		
	Percentage (%)	64.5	12.6	7.9	5.6	3.6	2.2	1.5	0.9	0.8	0.4			
	Cumulative percentage (%)	64.5	77.1	85.0	90.6	94.2	96.4	97.9	98.8	99.6	100.0			

Fig. 1. Table R1. See the caption for Table R1 in C11.

C13
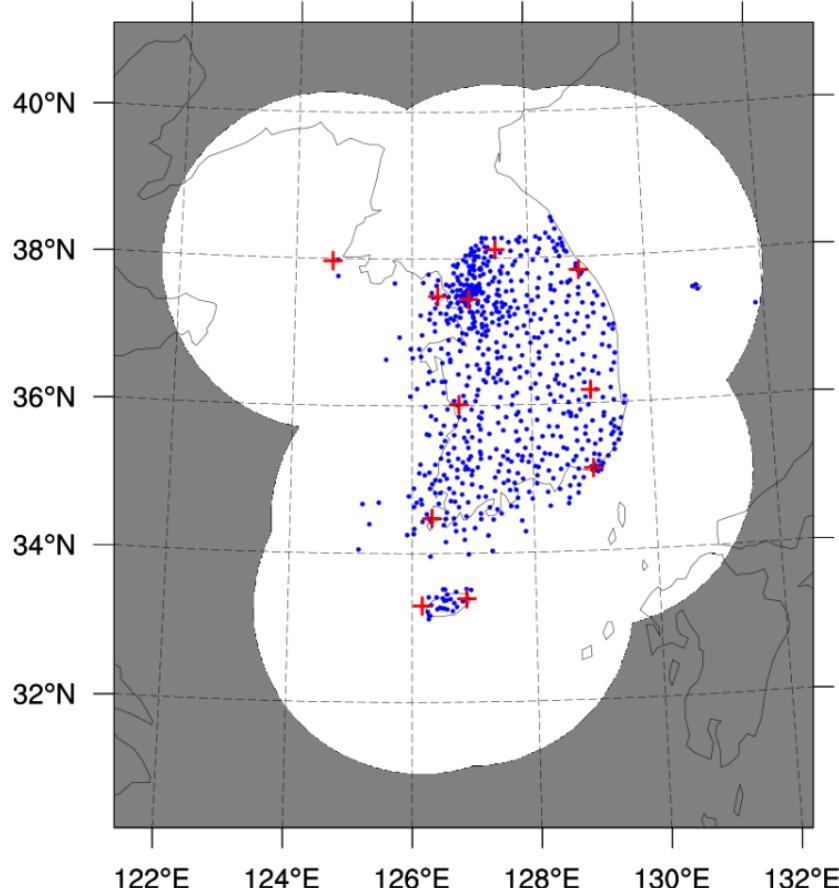
Fig. 2. Figure R1. See the caption for Figure R1 in C11.